High Temperature Nanoindentation Response of RTM6 Epoxy Resin at Different Strain Rates

P. Frontini, S. Lotfian, M. A. Monclús & J. M. Molina-Aldareguia

Experimental Mechanics
An International Journal

ISSN 0014-4851

Exp Mech
DOI 10.1007/s11340-015-9985-4

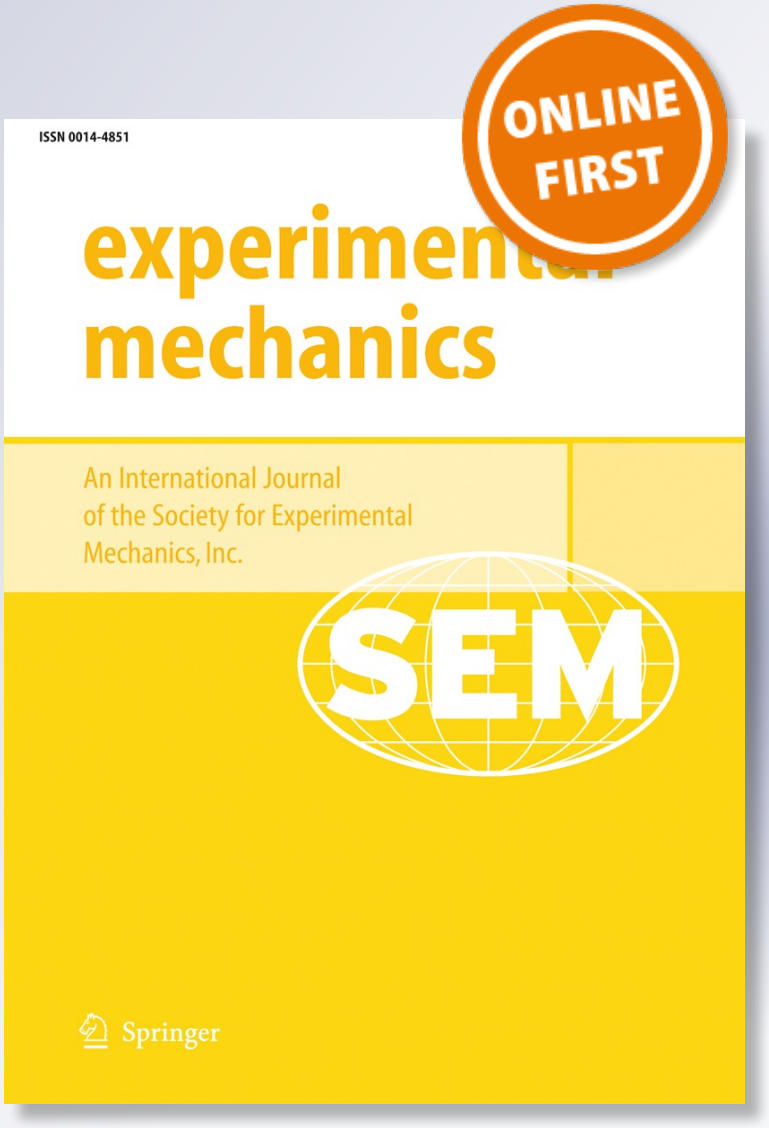

Springer

Experimental Mechanics
DOI 10.1007/s11340-015-9985-4

High Temperature Nanoindentation Response of RTM6 Epoxy Resin at Different Strain Rates

P. Frontini · S. Lotfian · M.A. Monclús · J.M. Molina-Aldareguia

Received: 10 February 2014 / Accepted: 12 January 2015

Abstract This paper explores the feasibility of characterizing the mechanical response of the commercial aerospace grade epoxy resin RTM6 by nanoindentation tests at varying temperatures and strain rates. Since glassy polymers exhibit time-dependent mechanical properties, a dynamic nanoindentation technique was used. This method consists on superimposing a small sinusoidal force oscillation on the applied force. Viscoelastic properties are then characterized by their storage and loss moduli, whereas the visco-plastic response of the material can be associated to its hardness. In such experiments, thermal stability of the measuring technique is critical to achieve a low thermal drift and it becomes increasingly important as the measuring temperature increases. Our results show that conventional methods applied for drift correction in nanoindentation of inorganic materials are not applicable to glassy polymers leading to physically inconsistent results. We propose a method for drift correction based on the hypothesis that viscoelastic modulus should be a function of the applied load and frequency but independent of the global strain rate. Using this method, it was possible to determine the viscoplastic properties of RTM6 between RT and 200 °C.

P. Frontini (✉)
Instituto de Investigaciones en Ciencia y Tecnología de Materiales (INTEMA), Facultad de Ingenieria, Universidad Nacional de Mar del Plata, Av. J. B. Justo 4302, B7608FDQ Mar del Plata, Argentina
e-mail: pmfronti@fi.mdp.edu.ar

P. Frontini · S. Lotfian · M.A. Monclús · J.M. Molina-Aldareguia
IMDEA Materials, C/ Eric Kandel, 2, Tecnogetafe, 28906 Getafe, Madrid, Spain

Keywords High temperature nanoindentation · Epoxy resins · Drift effects

Introduction

Instrumented indentation technique, also known as nanoindentation or depth sensing indentation can be used to measure mechanical properties, such as Young's modulus and hardness, at the micro and nano-scale [1]. Its high spatial resolution and depth sensitivity allow measuring the variations in the local mechanical properties of nano and microcomposites, which constitutes the basis for multiscale optimization of mechanical properties of many advanced materials [2].

Instrumented indentation techniques have been generally developed for room temperature. Nevertheless, in the last few years, there has been an increasing demand for conducting nanoindentation tests under relevant service temperatures. In order to get reliable measurements, high-temperature nanoindentation requires high thermal stability, since thermal drift can have a large effect on the measured displacements, which are usually in the nanometer range. Driven by this, many improvements have been made to both instrumentation and methods by the leading manufacturers, and with some of the current commercial models, it is now possible to derive local mechanical properties at service temperature.

Most of the work up to date on high temperature nanoindentation has focused on inorganic materials. However, this capability might be very valuable for testing epoxy resins used in carbon fiber reinforced plastics (CFRP) for aerospace applications, that work in very harsh environments (temperature changes, radiation, moisture ….) that promote hygrothermal

Published online: 27 January 2015

aging. Hygrothermal aging typically refers to the deterioration of the performance of a material due to prolonged exposure to moisture and variable temperature conditions (http://ntrs.nasa.gov/archive/nasa/casi.ntrs.nasa.gov/20090023547_2009022929.pdf) [3–5]. The ability to measure the local mechanical properties by nanoindentation would allow determining the hygrothermal aging suffered by the resin in real CFRP subjected to service conditions [6].

To this end, nanoindentation tests should allow extracting relevant material parameters for the calibration of constitutive models that describe the mechanical response of polymers. Contrary to most inorganic materials, the deformation of polymeric materials is inherently time dependent. Their viscoelastic properties are characterized by their storage and loss moduli, whereas the visco-plastic response of the material can be associated to its strain-rate dependent hardness [7–10]. This implies performing tests at a wide range of temperatures and strain rates.

Despite of its inherent importance, the nanoindentation of rigid polymeric materials at elevated temperatures is still an emerging discipline [11, 12]. There is very scarce literature regarding the characterization of glassy polymers at varying temperatures and strain rates via nanoindentation, counting mainly on a few reports covered by the leading indentation equipment manufacturers (http://www.hysitron.com/LinkClick.aspx?fileticket=ByGFq9XtNDg%3d&tabid=330) (http://www.nanovea.com/Application%20Notes/temperature-anoindentation.pdf) (http://www.micromaterials.co.uk/wp-content/uploads/2013/01/mm-polymeric.pdf) [13]. Moreover, generally none have addressed a multiscale characterization approach in order to predict macroscopic behavior from property determination at local scales [14–16]. For high temperature indentation testing, it is necessary to have a very stable thermal environment so as to minimize effects due to temperature changes.

In this paper, we investigate the response to dynamic indentation of commercial aerospace grade epoxy resin RTM6 as a function of temperature in the glassy regime. RTM 6 is a monocomponent epoxy resin which was specifically developed to fulfill the requirements of the aerospace and space industries in advanced resin transfer moulding (RTM) processes. It is a premixed epoxy system suitable for service temperatures up to 180 °C. The paper shows that conventional drift correction methods do not work well on these materials due to their time-dependent properties. Instead, an alternative method that combines dynamic indentation with high temperature testing to correct for spurious drift effects is proposed.

Background

Characterization of polymers by indentation has always been challenging because these materials exhibit strong temperature and time-dependent mechanical properties. Viscoelasticity of polymers manifests itself even at room temperature.

During an indentation test under varying loading conditions, polymers exhibit a marked creep behavior, which acts during the whole loading history. It manifests itself mainly during the dwell phase and may be observed also at the unloading portion of the load–displacement (P-h) curve. Hardness and modulus are affected by creep because the slope of the P-h curve computed from the upper part of the unloading curve, following the standard Oliver and Pharr (O&P) method [1], contains not only elastic but also viscoelastic-viscoplastic contributions. If these phenomena appear, in the worst case, the indentation depth can increase even when the indenter is unloaded and a characteristic nose appears at the beginning of the unloading curve rendering an abnormally high (and even negative) contact stiffness, resulting in erroneous calculation of Young's modulus and/or hardness.

Creep influence in polymer indentation is usually taken into account and corrected by holding the indenter at maximum load for a long time resulting in a negligible residual creep rate compared with the unloading rate [17]. This technique allows short-lived creepy materials to accommodate to the load. However, this strategy cannot be used aiming to determine the strain-rate-dependent properties of materials using self similar-indenters, since the strain-rate dependency will be erased during the dwell period.

An alternative method that can be used in time-dependent polymers is based on superimposing a small oscillating ac force on the primary dc load on the indenter during indentation and measuring the phase and relative amplitude of the indenter-sample contact response by a lock-in amplifier, which can then be used to determine the viscoelastic properties of the material - storage modulus (E'), loss modulus (E'') and tan δ (E''/E') [15, 17–23]. This method is referred to as dynamic indentation and has been given different names depending on the instrument manufacturer (*Continuous Stiffness Measurement* (CSM) (Agilent), *Dynamic compliance Testing* (Micro Materials) or *Nano-DMA* (Hysitron)). Extraction of accurate material properties with this method relies on an appropriate model for the dynamic response of the indentation system and on the application of a suitable constitutive equation. The sample is usually represented by a parallel spring and dashpot arrangement (Kevin-Voigt cell), as this reduces the complexity of any mathematical analysis involved to deconvolute the instrument response function from the measured data. Other more complicated models (i.e. adding elements to the simple Kevin-Voigt model), can be required to successfully obtain loss/viscosity parameters.

Since polymer properties are time-dependent, the use of experimental techniques with very high thermal stability is required so that the results are not discredited by the inherent

error caused by thermal drift of the measuring device. Drift rates might vary in a relatively short time; therefore they must be monitored and corrected for each test. Unfortunately, *conventional* methods that are typically used for correcting drift effects rely on measuring drift rates either at the initial contact or at the end of the unloading process, by maintaining a small load for a dwell period and recording the displacement. On inorganic materials, these conventional methods work well because any displacement recorded during this hold period can only be attributed to spurious drift effects. In this paper, we will show that they are not applicable in glassy polymers because substantial creep effects might take place during these hold periods, giving rise to the incorrect determination of drift rates. This paper uses an alternative approach to correct for drift in glassy polymers based on dynamic nanoindentation, referred to as *reference* drift correction method. The method is successfully applied to determine visco-plastic parameters of RTM6, an aeronautical grade epoxy resin.

Experimental Procedure

Material

Sample tests were conducted on a Hexcel® HexFlow® RTM 6 Epoxy System for Resin Transfer Moulding Monocomponent System (T_g=190 ° C), which was cured according to the corresponding manufacturers' instructions.

Surface preparation was performed by mechanical grinding using silicon carbide papers of progressively finer grade (between 320 and 2400) with water lubrication and final polishing using 1, 0.3 and 0.02 μm alumina particle size aqueous suspensions on velvet cloths (NAP Struers). The surface thus obtained had a roughness (R_a) of $\approx$ *1 nm* according to AFM measurements (see Fig. 1), which provides a smooth surface for nanoindentation tests. Samples with a thickness of $\approx$ 500 μm were used in order to avoid temperature gradients across the sample thickness during high temperature nanoindentation. This is very important in glassy polymers due to the large temperature dependency of Young modulus and their low thermal conductivity. Large differences between the top and bottom temperature might lead to a rigid/compliant system leading to serious compliance contributions in the measurement from the bottom part of the sample, especially close to T_g. The samples were mounted on metal discs, using a high temperature adhesive (MINCO, Forta Fix, AUTOSTIC FC 6 250 ml). Surface temperature was monitored by placing a thermocouple onto the sample surface.

Despite using thin specimens, a distinct gap between the temperature set point of the heating platform and the measured surface temperature was found, which varied between 10 and 50 °C, depending on testing temperature. The maximum testing temperature was limited to 200 °C, at which point the color of the sample changed dramatically due to thermal degradation (see Fig. 2).

Dynamic Mechanical Spectroscopy (DMA)

RTM6 resin were characterized by dynamic mechanical thermal analysis. Oscillatory torsion tests at a frequency of 1 Hz and strain amplitude of 0.02 % were performed using an Anton Paar MCR 301 rheometer equipped with CTD 600 thermostatic air convection chamber. A heating rate of 5 °C/min was applied on prismatic samples with nominal dimension of 15×9.8×2 mm^3. Shear storage modulus G', shear loss modulus G' and los factor *tan* δ, were recorded as a function of temperature (−60 to 250 °C) . Additionally, DMA spectra was also determined under oscillatory bending mode using a single-cantilever clamp in a Q800 DMA analyzer. Tests were performed on prismatic samples with nominal dimension of 26×10.0×1.6 mm^3 with a span of 50 mm at a frequency of 1 Hz, at a strain amplitude of 30 μm, and applying a heating rate of 3 °C/min. Storage modulus E' was recorded over a temperature range of 23 to 300 °C. Results are shown in Fig. 3(a), (b) and (c).

NanoIndentation Testing

Nanoindentation testing was carried out on a Hysitron TI950 Triboindenter equipped with the nanoDMA III option (http://www.hysitron.com/products/ti-series/ti-950-triboindenter). The sample was mechanically clamped on a heating stage that allows heating at temperatures up to 400 °C. The nanoDMA option allows the application of an oscillatory load superimposed to the main quasi-static dc load, for the continuous measurement of hardness, storage and loss moduli, and tan δ, as a function of depth, frequency and time. In this method, described in detail by Oliver and Pharr [24], the kinematic model of the system, based on a damped harmonic oscillator, is used to relate the stiffness (S) and the damping (D) of the contact, to the phase and amplitude response. The reduced storage and loss modulus (E_r' and E_r'') and hardness (H) are then derived as a function of indentation depth (h) through the equations of the contact:

$$E_r^{'} = \frac{S\sqrt{\pi}}{2\sqrt{A(h)}}\left(1-\nu_{sample}{}^2\right) \tag{1}$$

$$E_r^{''} = \frac{D\omega\sqrt{\pi}}{2\sqrt{A(h)}}\left(1-\nu_{sample}{}^2\right) \tag{2}$$

$$H = \frac{F}{A(h)} \tag{3}$$

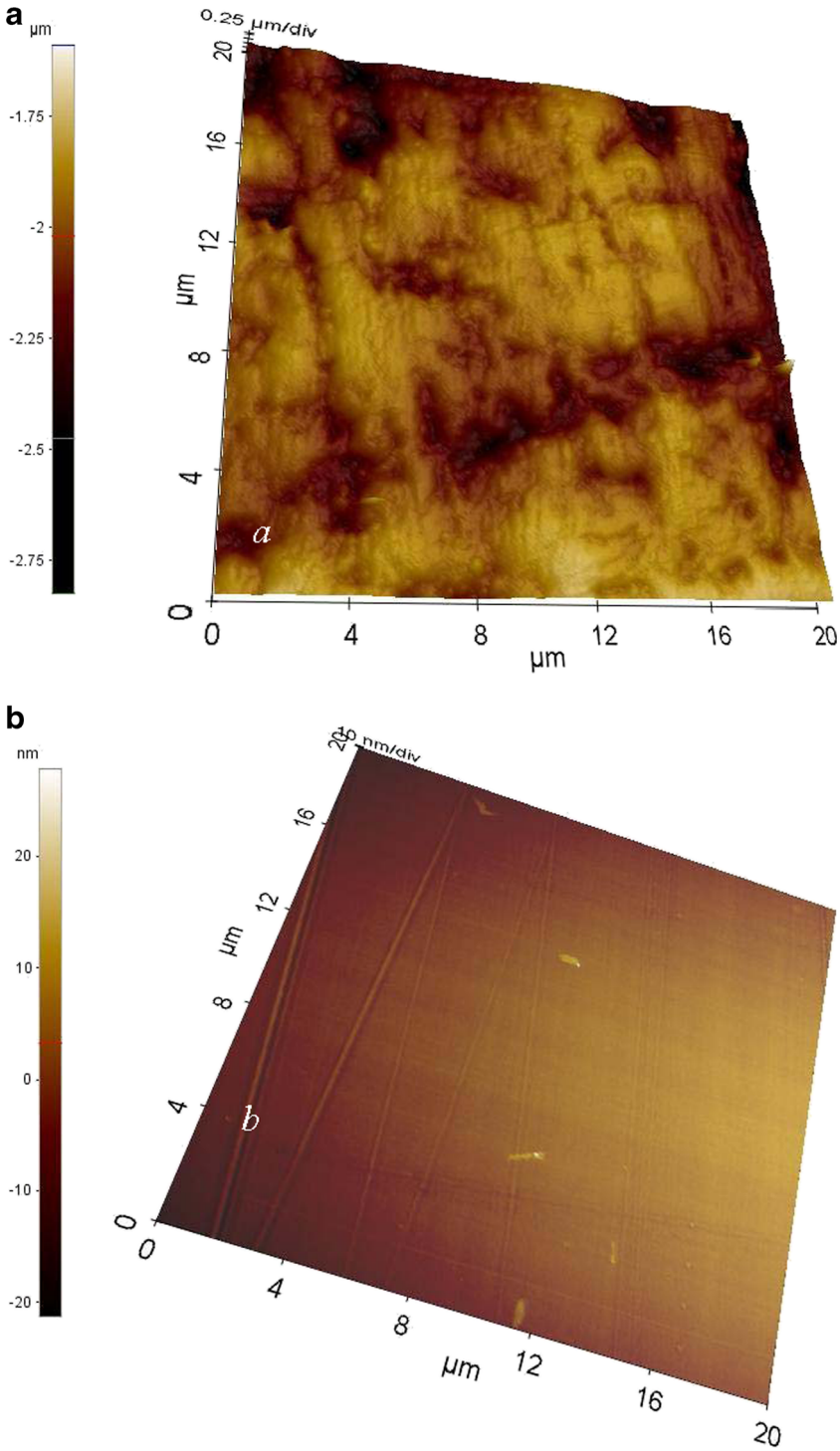

Fig. 1 Surface before polishing (**a**). Surface after polishing (**b**)

where the contact area $A(h)$ is obtained from the tip area function, which was calibrated beforehand from indentations on fused silica; ω is the oscillation frequency, and ν is the Poisson's ratio of the test material.

As elastic displacements occur both in the specimen (with modulus of elasticity E_{sample} and Poisson's ratio ν_{sample}) and in the indenter, the elastic modulus of the sample is calculated from the reduced modulus, E_r using

$$E_{sample} = \left(1-\nu_{sample}{}^2\right) / \left(\frac{1}{E_r} - \frac{1-\nu_{indenter}{}^2}{E_{indenter}}\right) \quad (4)$$

Fig. 2 Change in color of the RTM6 sample after heating to 200 °C (from *yellow* to *dark brown*)

Assuming $E_{diamond}$=1141 GPa, $\nu_{diamond}$=0.07 and ν_{epoxy}=0.35

The oscillation frequency was set to 200 Hz with variable force amplitude in order to attain oscillation amplitudes of ≈ 1–2 nm. The maximum DC force was varied between 5.5 and 6 mN, depending on testing conditions, in order to reach maximum indentation depths of ≈ 1 μm. Indentation tests were carried out at prescribed indentation strain rates of 0.25, 0.05 and 0.01 s^{-1}, using a three-side pyramidal (Berkovich) diamond indenter. The indentation strain rate $\left(\dot{\varepsilon}\right)$ is given by equation (5), where $\dot{h}$ is the indenter displacement velocity, and h is the depth [25].:

$$\dot{\varepsilon} = \frac{\dot{h}}{h} \tag{5}$$

Indentation tests were performed at 8 different temperatures 25, 50, 70, 80, 115, 140, 165 and 200 °C. For all indentation tests, an initial contact load of 2 μN was maintained constant for a period of 60 s and the displacement monitored over time. This segment is conventionally used in indentation to compute the drift rate prior to the test from the last 30 s of the hold segment. However, as will be shown in the results section, this approach leads to an incorrect determination of the drift rate, which was finally determined using the *reference* method described below.

Results and Discussion

Dynamic Mechanical Spectroscopy

Figure 3(a) and (b) show the temperature dependence of the shear storage modulus G' and the loss factor $tan\ \delta$ (G''/G'). The drops in the G' evolution and the peaks of the $tan\ \delta$ value characterize the physical transitions of the polymer. The main temperature damping of RTM6, occurs at T_g ~225 °C. It is associated to the glass transition involving long distance molecular motions. This relaxation is characterized by a very sharp drop of the G' storage modulus (about two decades). Moreover, the $tan\ \delta$ evolution shows that above 200 °C the viscous response of the polymer becomes significant (Fig. 3(b)). A small but distinct drop of G' can be noticed between 50 and 100 °C, which is related to a sub-*glass* transition. This type of wide dissipation peak is often exhibited by some epoxy systems at temperatures over room temperature. They are generally called T_ω in the specific literature [26, 27] and it is located between α and β − relaxation process. The particular temperature position of the maximum of $tan\ \delta$, corresponding to this relaxational process occurs approximately at 95 °C (T_ω~95 °C). This kind of relaxations has been already reported by other authors for RTM6 epoxy system specifically [28–32]. In the past, this additional relaxation was considered as a consequence of the structural or molecular arrangements within the network resulting from moisture absorption [30, 31]. Later investigations [32] associated this secondary viscoelastic transition with motions of the p-phenylene groups. Nevertheless, the precise ω-relaxation assessment in terms of molecular mobility remains still uncertain in literature [27] being its elucidation beyond the scope of the present paper. Consistently, the two drops in the storage modulus E' corresponding to the physical transitions of the polymer T_g and T_ω are also visible in Fig. 3(c).

Nanoindentation Tests Using the *Conventional* Drift Correction Method

In this section, we present the results of the *conventional* dynamic indentation tests. By *conventional*, we refer to the tests in which drift correction was carried out by measuring the drift rate during the initial contact at the beginning of the test, and correcting the data assuming a constant drift rate throughout the test. Figures 4 and 5 plot the storage modulus and hardness computed as a function of indentation depth at three different indentation strain rates (0.01, 0.05, 0.25 s^{-1}). For the sake of simplicity only plots for three selected temperatures (25, 90, 165 °C) are shown in this section, in which a detailed analysis of the load-penetration curves is presented. Complete results including all temperatures examined are presented later in a condensed form in Fig. 6 for the Storage Modulus and as an Eyring's Plot for Hardness data. The results show a large spread and a lack

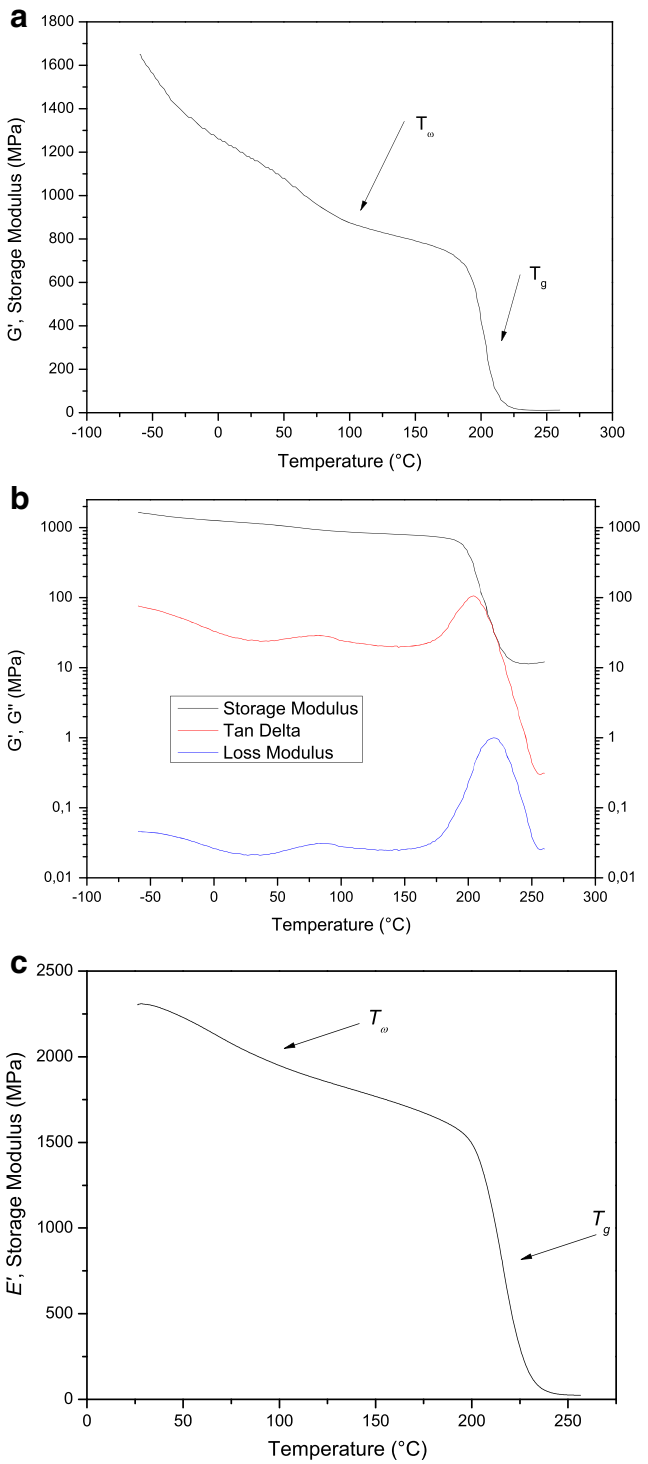

Fig. 3 Dynamic mechanical spectra of RTM6 epoxy resin: (**a**) Shear Storage Modulus vs. Temperature showing $\alpha-$ relaxation and ω-relaxation processes at $T_g \approx 225°C$ and $T_w \approx 95$ °C respectively; (**b**) Shear Storage Modulus (log), Shear Loss Modulus (log) and *Tan* δ (log) vs. Temperature; (**c**) Storage Modulus (log) vs. Temperature obtained in bending mode

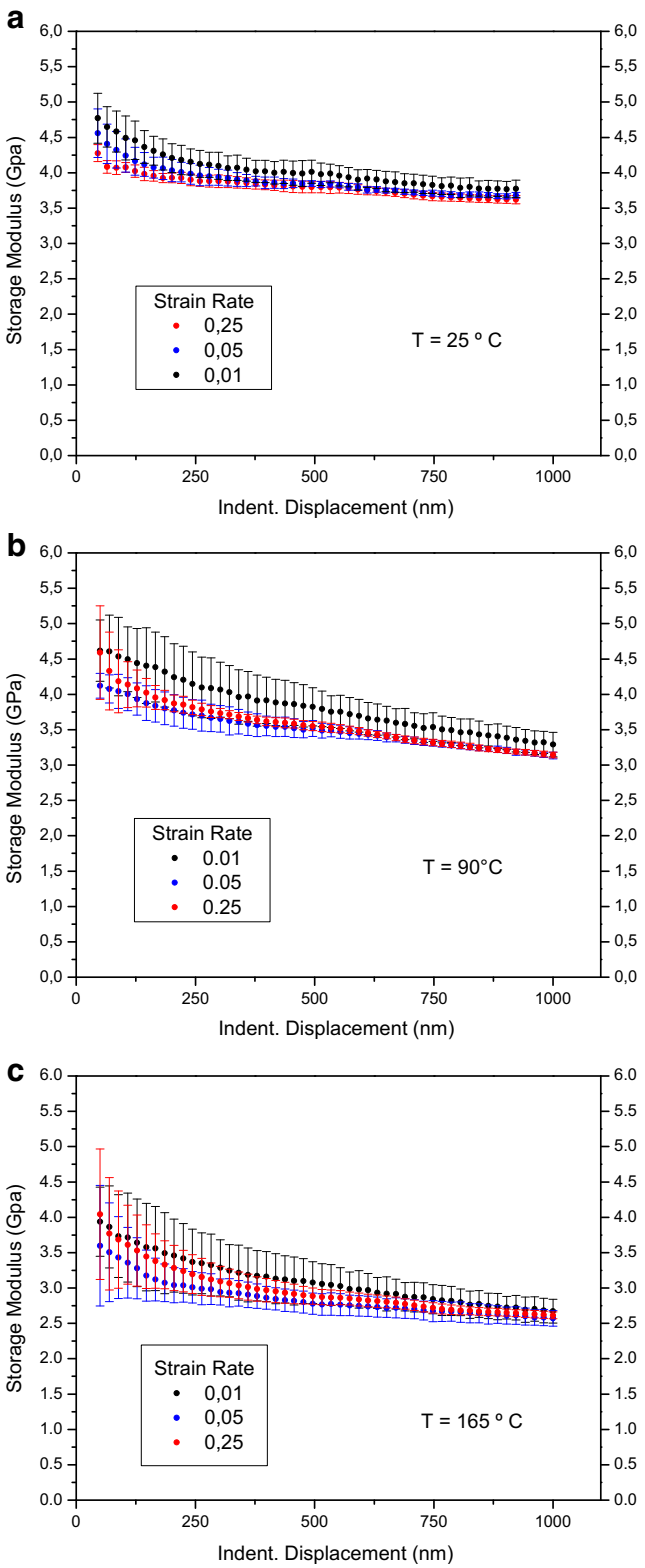

Fig. 4 Storage Modulus as a function of strain rate against indent displacement for three different temperatures. Values were corrected by the *conventional* drift rate determination used in conventional indenters. *Error bars* on the symbols represent one standard deviation

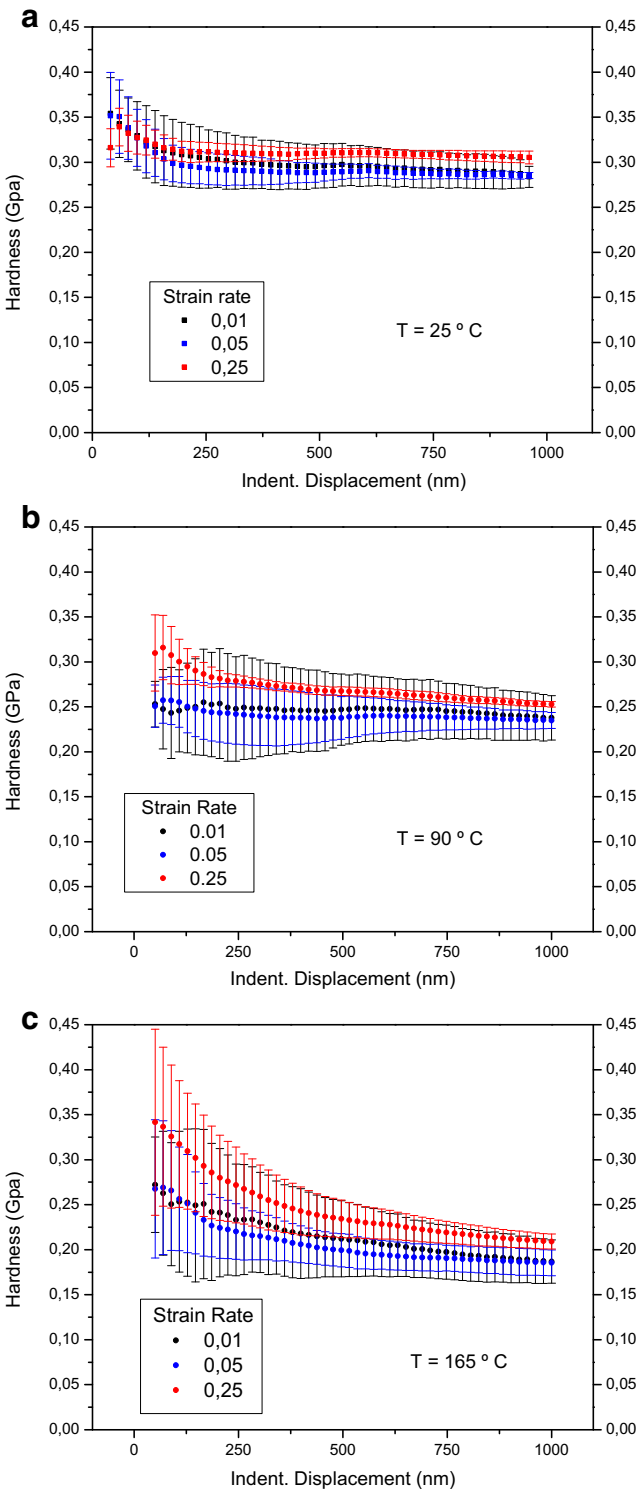

Fig. 5 Hardness as a function of strain rate against indent displacement for three different temperatures. Values were corrected by the conventional drift rate determination used in conventional indenters. *Error bars* on the symbols represent one standard deviation

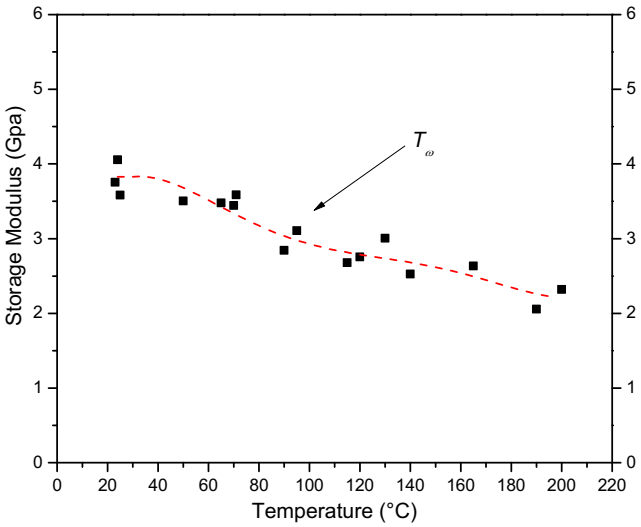

Fig. 6 Storage modulus as a function of temperature at 0.25 s-1 indentation strain rate. Plotted values were taken at 900 nm indentation depth. Data correspond to various runs, but *error bars* were omitted for clarity

of reproducibility in the measurements, particularly at low strain rates and high temperatures. The room temperature results show a plateau in storage modulus at indentation depths larger than ≈ 400 nm, with a value of 3.8 GPa, independent of indentation strain rate. The size effect encountered at shallow indentation depths for polymers is still under debate and has been attributed to different reasons, including sample preparation. However recent investigations performed on glassy polymers have revealed that the polymer surface stiffening mechanism is related to the creation of a mechanically unique interfacial region between the probe and the polymer surface [33]. The results are consistent with the expectation that storage modulus should be independent of indentation strain rate [34]. This suggests that *conventional* drift correction does a fair job at room temperature, presumably because thermal drift was relatively small (with typical values ranging from −0.05 to +0.1 nm/s).

For the lower strain rates, due to longer loading times, thermal drift effects become increasingly important and the data becomes more unreliable. In addition unlike the room temperature case, as testing temperature increased (Fig. 4(b) and (c)), the storage modulus did not saturate with indentation depth and the results were very scattered, especially at low indentation strain rates, giving rise to spurious storage moduli's dependency with indentation strain rate. It is worth mentioning that preliminary indentation tests performed on PC and PMMA (not shown here) under the same testing conditions presented the same features, thus suggesting that this behaviour is not particularly related with RTM6 epoxy resin itself. The drift rates determined at initial contact at 90 and 165 °C varied between −0.81 and +0.1 nm/s, giving much larger thermal drift oscillations than at room temperature and those obtained in the same machine when testing metals and ceramics in similar conditions. Errors in drift estimations arise from the viscoelastic-viscoplastic behavior of the polymers themselves, which make traditional drift determination methods unpractical, as the polymer reacts by deforming over

time (even at the small applied initial contact load of 2 μN), especially at higher temperatures. Incorrect drift determination and correction affects more the data obtained at low indentation strain rates, for which the test lasted up to 250 s, thus explaining their larger scatter.

The same spurious effects of the wrong drift estimation can be found when the hardness is plotted in Fig. 5, which illustrates the hardness profiles obtained at different temperatures as a function of strain rate. The hardness was fairly constant at depths greater than ~400 nm, but again results showed a large scatter, especially at low indentation strain rates. In these circumstances, the variation in hardness with indentation strain rate is far from the expected behaviour of the RTM6 epoxy's strain rate sensitivity [35].

Nanoindentation Tests Using the *Reference* Method for Drift Correction

In this section, we present an alternative analysis carried out in the data presented above to avoid the errors associated with *conventional* drift correction methods in polymeric materials. The analysis relies on mainly two hypotheses: (1) drift effects are negligible at the largest indentation strain rate of 0.25 s^{-1} and (2) storage modulus should remain constant and independent of strain rate at each temperature.

The first hypothesis is reasonable as the total indentation time for a 1000 nm deep indent at the prescribed strain rate of 0.25 s^{-1} is 17 s; therefore, it is safe to assume that, for the measured machine drift rates of < 0.1 nm/s, thermal drift effects will not be significant.

Regarding the second hypothesis, it is accepted that the storage modulus should be independent of the penetration rate and should only be a function of the frequency and temperature applied [34].

Comparison of Computed Storage Modulus with DMA Spectroscopy

To weight the validity of the first hypothesis, Fig. 6 plots the storage modulus determined from indentation tests carried out at a strain rate of 0.25 s^{-1}, as a function of temperature. No drift correction was applied to these data and a Poisson ratio of 0.35 was assumed for RTM6 at all temperatures (specified after equation 4). These results may be compared with tensile (Young's) modulus values and DMA results.

Quantitatively speaking, the average modulus value of 3.5–4.0 GPa obtained by nanoindentation at room temperature is larger than the 2.9 GPa reported for the Young's modulus of RTM6 resin (http://www.hexcel.com/Resources/DataSheets/RTM-Data-Sheets/RTM6_global.pdf). This finding is consistent with the general trend reported for indentation measurements in polymers [18]. This is also true when comparing the indentation storage modulus with the storage modulus E' obtained from DMA spectroscopy (2.3 GPa from Fig. 3(c)). In this case, an additional factor affecting the mismatch between the absolute values of the elastic moduli

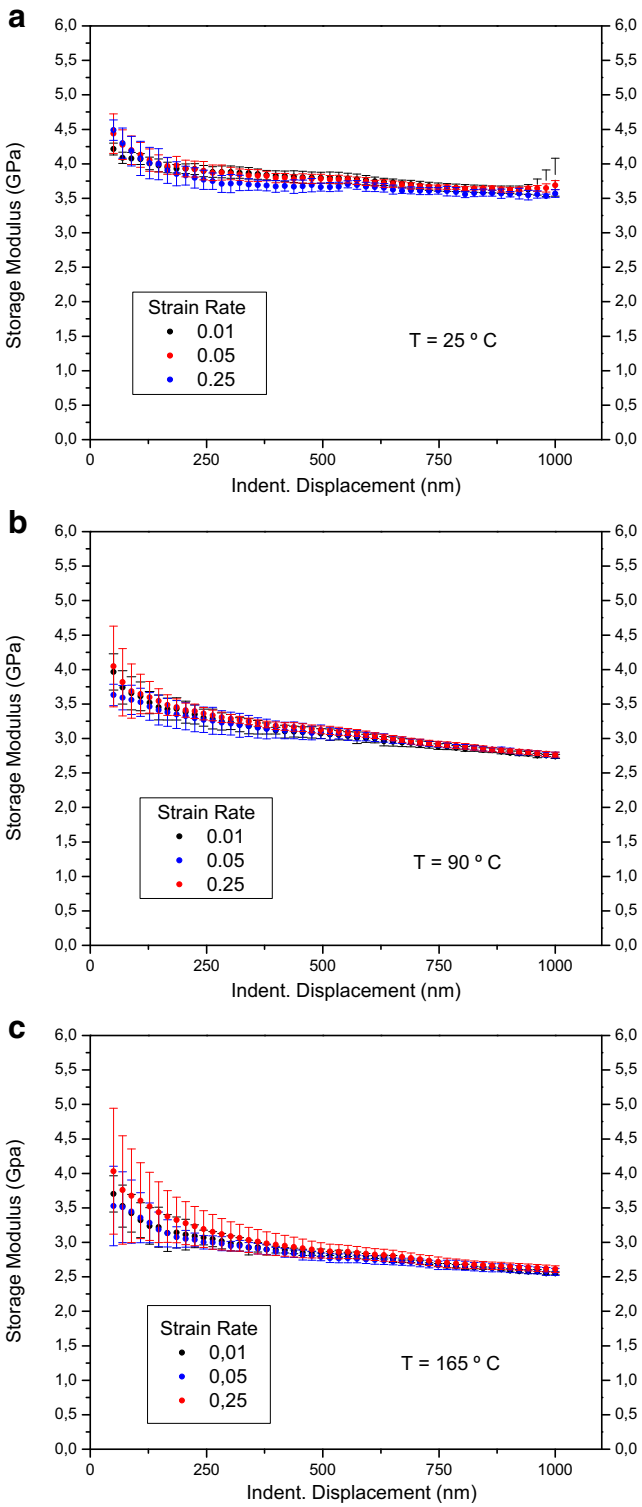

Fig. 7 Storage Modulus as a function of strain rate against indent displacement after reference drift correction for three different temperatures. *Error bars* on the symbols represent one standard deviation

determined from both methods could be the fact that, in DMA, data were obtained at a much lower superimposed frequency (1 Hz vs. 40 Hz) and in the linear viscoelasic regime.

Nevertheless, and from a qualitatively viewpoint, the trends observed in storage modulus with temperature for DMA (Fig. 3(c)) and for nanoindentation (Fig. 6) are remarkably similar, corroborating the validity of the first hypothesis.

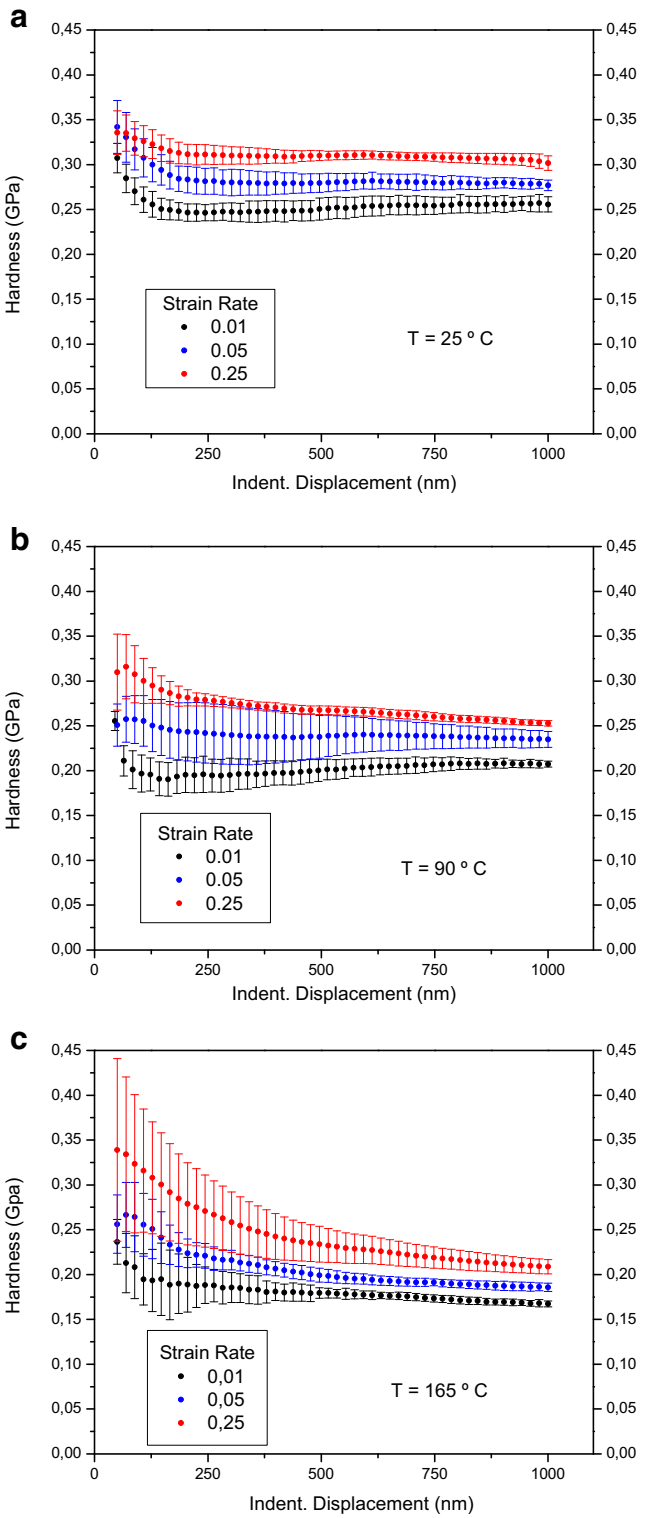

Fig. 8 Hardness as a function of strain rate against indent displacement after reference drift correction for three different temperatures. The *error bars* correspond to one standard deviation

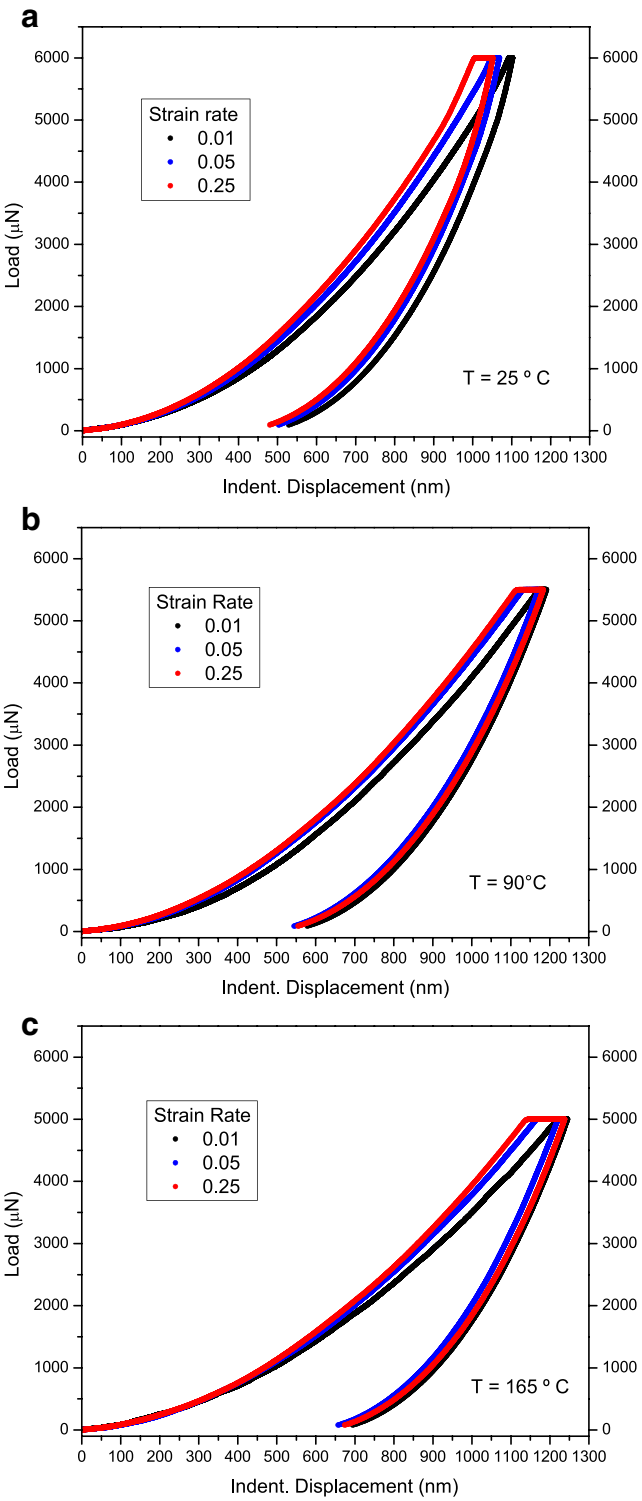

Fig. 9 Inferred Load - indent displacement plots after reference drift correction for three different temperatures

Worth mentioning is the fact that the nanoindentation data in Fig. 5 is able to capture the smooth drop of the storage modulus E′ between 50 and 120 °C associated with the T_ω transition reported in Fig. 3(c). Given the profound differences in test method and sample geometry, the agreement with DMA is promising.

Application of the *Reference* Method for Drift Correction

Considering that the conventional drift correction method led to physically inconsistent results (see Figs. 4 and 5), the curves corresponding to the two lower indentation strain rates used i.e. 0.05 and $0.01s^{-1}$ were no longer corrected for drift rate monitored by the instrument at the beginning of the test. Instead the *reference* method was applied. This method relies on the second hypothesis mentioned at the beginning of section "Nanoindentation Tests using the *reference* method for drift correction", i.e., that the storage modulus should remain constant and independent of indentation strain rate at each temperature, provided that tests are performed at the same superimposed oscillation frequency [34]. Accordingly, the storage modulus vs. penetration curves obtained at the fastest strain rate, i.e., $0.25s^{-1}$ (and hence marginally affected by drift effects) were taken as reference for each temperature. Each individual load penetration curve obtained for the lower indentation rates of 0.05 and $0.01s^{-1}$ was then corrected using the drift rate determined by imposing the same reference storage modulus vs. penetration depth curve obtained at $0.25s^{-1}$, at every temperature. Figures 7 and 8 display the storage modulus and hardness for the three strain rates corresponding to the three selected temperatures (25, 90 and 165 °C) after the application of the *reference* drift correction method to the raw indentation data (originally shown in Figs. 4 and 5). The applied correction leads to hardness results that give rise to a clear increasing trend of hardness with strain rate at all temperatures tested, as expected.

Analysis of Corrected Hardness Data: Eyring's Plot

The stress–strain response of most amorphous polymers is known to be dependent on temperature and strain rate. Accordingly, the load–displacement curves obtained after the *reference* drift correction (Fig. 9) show the expected tendency with strain rate and temperature relative to the mechanical response of glassy polymers providing additional support to the validity of the proposed correction. At a fixed testing temperature, load- displacement curves show a clear influence of the strain rate. A higher loading rate yielded a higher load for the same displacement into the surface.

The curves also exhibit creep at maximum indentation loads during the hold period of 5 s, as well as a pseudo-elastic behavior on unloading irrespectively of the original loading rate.

From the viewpoint of potential applications, a simple correlation of indentation hardness to macroscopic mechanical parameters is of growing interest in the polymer field since this may offer interesting possibilities with respect to quality control of load-bearing polymer products [36]. For metals with almost fully plastic deformation behavior, an excellent correlation between hardness and yield stress already exists as it was shown by Tabor [37]. In the case of polymers a straightforward correlation has not being yet postulated since the ratio of hardness to yield stress highly depends on the deformation behavior itself and loading mode [36]. However in the case of shear-controlled deformation behavior, and this is the case of thermoset resins, such correlations are possible and comparable with Tabor's relationship for metals [36].

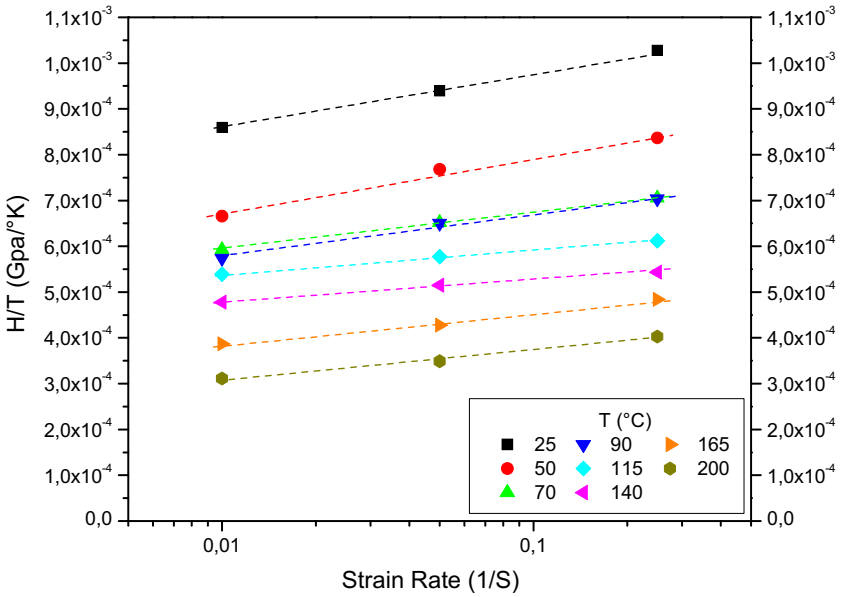

Fig. 10 Eyring plot constructed from corrected indentation hardness divided by absolute temperature (H/T) against logarithm strain rate. Data correspond to various runs, but *error bars* were omitted for clarity

In most cases, the yield stress obeys thermally activated processes following the well known Eyring's model [5], and this has been corroborated in epoxy resins [6]. Eyring's model proposes a linear relationship between yield stress divided by the absolute temperature and the logarithmic strain rate, displaying the same slope for each particular temperature. In an attempt to prove whether the applied correction is robust or not, the corrected hardness data collected for the eight tested temperatures were plotted according to Eyring's model as shown in Fig. 10. The plot shows that the corrected indentation hardness over temperature (*H/T*) data fall into straight lines, following the same stress-activated Eyring flow model than the yield stress data for epoxy resins and confirming the good correlation between yield stress and hardness for epoxy resins over a wide range of temperatures and strain rates.

An abnormal behavior was displayed by experiments performed at temperatures within the T_ω transition region, where the data scatter was also larger. Data points obtained at 70 °C practically overlap with the data determined at 90 °C (see Fig. 10). It has been noticed previously [27, 38] that thermal ageing may affect the ω-relaxation process in the temperature range where it appears. Indeed this effect may explain the apparent abnormal behavior found in this regime, if we consider that the sample was being thermally aged during the experiment itself. Thermal aging involves the simultaneous reduction of free volume and conformational changes of the crosslinked molecular structure when exposed to sub-*Tg* temperatures for extended periods of time.

Yielding of thermosets and thermoplastics is similar and is usually controlled by T_g. However if a secondary molecular motion, distinct from molecular processes of the α-transition exists, it may exert an independent contribution to the macroscopic yielding. Annealing close to secondary relaxation transitions usually leads to an increase of the yield stress [39, 40].

Conclusions

In the present study, the effect of strain rate on the hardness and storage modulus of an RTM6 aeronautical epoxy resin has been experimentally explored by dynamic nanoindentation at high temperatures. Tests were performed at eight temperatures between RT and 200 °C at three different indentation strain rates (0.01, 0.05, 0.25 s^{-1}) .

The storage modulus determined by nanoindentation at 0.25 s^{-1} were comparable to the results obtained by DMA spectroscopy within the temperature range scanned. The measurements appear to be sensitive enough to detect subtle T_ω transitions at temperatures below T_g. It was made clear that *conventional* drift correction routines hindered the real response of material, especially at lower indentation strain rates. To overcome this problem, the load–displacement curves were corrected for drift by applying a novel *reference* correction method that relies on two hypothesis: (1) machine drift rates are sufficiently low to render drift correction unnecessary for the fastest strain rate ($0.25 s^{-1}$) and (2) storage modulus should only be a function of temperature and dynamic frequency, and independent of indentation strain rate. The robustness of the proposed method was confronted by plotting the corrected hardness data in an Eying plot. The expected linear behavior was confirmed, supporting the validity of the method. Future work is in progress in order to derive the multiaxial viscoelastic-viscoplastic constitutive equations representing global mechanical behavior, by using the *reference* drift corrected load–displacement plots.

Acknowledgments The authors want to acknowledge Xavier Morelle, PhD sudent at Université catholique de Louvain - Institute of Mechanics, Materials and Civil Engineering (iMMC) for providing epoxy samples, and Dr. Juan Pedro Fernández from IMDEA and Ulises Casado from INTEMA for performing DMA measurements. P. M. Frontini was recipient of a sabbatical stay fellowship from Ministerio de Educación y Ciencia (Spain).

References

1. Oliver WC, Pharr GM (1992) An improved technique for determining hardness and elastic-modulus using load and displacement sensing indentation experiments. J Mater Res 7(6):1564–1583
2. Kim JH, Ko JH, Bae B-S (2007) Dispersion of silica nano-particles in sol–gel hybrid resins for fabrication of multi-scale hybrid nanocomposite. J Sol–gel Sci Technol 41(3):249–2551
3. Lin YC, Chen X (2005) Investigation of the effect of hygrothermal conditions on epoxy system by fractography and computer simulation. Mater Lett 59(29):3831–3836
4. Couture A, Laliberte J, Li C (2013) Mode I fracture toughness of aerospace polymer composites exposed to fresh and salt water. Chem Mater Eng 1(1):8–17
5. Miller SG, Roberts GD, Bail JL, Kohlman LW, Binienda WK (2012) Effects of hygrothermal cycling on the chemical, thermal, and mechanical properties of 862/W epoxy resin. High Perform Polym 24(6):470–477
6. Llorca J, González C, Molina-Aldareguía JM, Segurado J, Seltzer R, Sket F, Rodríguez M, Sádaba Muñoz R, Canal LP (2011) Multiscale modeling of composite materials: a roadmap towards virtual testing. Adv Mater 23:5130–5147
7. Richeton J, Ahzi S, Vecchio KS, Jiang FC, Makradi A (2007) Modeling and validation of the large deformation inelastic response of amorphous polymers over a wide range of temperatures and strain rates. Int J Solids Struct 44:7938–7954
8. Anand L, Ames NM (2006) On modeling the micro-indentation response of an amorphous polymer. Int J Plast 22:1123–1170
9. Jordan JL, Foley JR Siviour CR (2008) Mechanical properties of Epon 826/DEA epoxy. Mech Time-Depend Mater 12:249–272
10. Zhang CY, Zhang YW, Zeng KY, Shen L (2006) Characterization of mechanical properties of polymers by nanoindentation tests. Philos Mag 86(28):4487–4506
11. Gray A, Orchid D, Beake BD (2009) Nanoindentation of advanced polymers under non-ambient conditions: creep modelling and tan delta. J Nanosci Nanotechnol 9(7):4514–4519

12. Lu YC, Jones DC, Tandon GP, Putthanarat S, Schoeppner GA (2010) High temperature nanoindentation of PMR-15 polyimide. Exp Mech 50:491–499
13. http://cp.literature.agilent.com/litweb/pdf/5990-5761EN.pdf (2010) Nanoindentation, Scratch, and Elevated Temperature Testing of Cellulose and PMMA Films . Agilent Technologies Application Note, 2010
14. Seltzer R, Kim J, Mai YW (2011) Elevated temperature nanoindentation behaviour of polyamide 6. Polym Int 60:1753–1761
15. Kranenburg JM, Tweedie CA, van Vliet KJ, Schubert US (2009) Challenges and progress in high-throughput screening of polymer mechanical properties by indentation. Adv Mater 21:3551–3561
16. Rodríguez M, Molina-Aldareguía JM, González C, Llorca J (2012) Determination of the mechanical properties of amorphous materials through instrumented nanoindentation. Acta Mater 60:3953–3964
17. Van Landingham MR (2003) Review of instrumented indentation. J Res Natl Inst Stand Technol 108:249–265
18. Beyaoui M, Mazeran PE, Arvieu MF, Igerelle M, Guigon M (2009) Analysis of nanoindentation curves in the case of bulk amorphous polymers. Int J Mater Res 100:1–7
19. Hay J, Herbert E (2010) Measuring the complex modulus of polymers by instrumented indentation testing. Exp Tech. doi:10.1111/j.1747-1567.2010.00618.x
20. VanLandingham MR, Villarrubia JS, Guthrie WF, Meyers GF (2001) Nanoindentation of polymers: an overview. Macromol Symp 167:15–43
21. Odegard GM, Gates TS, Herring HM, Chakravartula A, Komvopoulos K (2005) Characterization of viscoelastic properties of polymeric materials through nanoindentation. Exp Mech 45(2):130–136
22. Chakravartula A, Komvopoulos K (2006) Viscoelastic properties of polymer surfaces investigated by nanoscale dynamic mechanical analysis. Appl Phys Lett 88(13):131901–131903
23. Hayes SA, Goruppa AA, Jones FR (2004) Dynamic nanoindentation as a tool for the examination of polymeric materials. J Mater Res 19(11):3298–3306
24. Oliver WC, Pharr GM (2004) Measurement of hardness and elastic modulus by instrumented indentation: advances in understanding and refinements to methodology. J Mater Res 19(1):1–20
25. Fisher-Cripps C (2004) Nanoindentation, 2nd edn. Springer, New York, p 146
26. Pascault J-P (2002) In: Pascault J-P, Sautereau H, Verdu J, Williams RJJ, Deker M (ed) Thermosetting polymers (plastics engineering) 1st ed. New York, p 339
27. Colombini D, Martinez-Vega JJ, Merle G (2002) Influence of hydrothermal ageing and thermal treatments on the viscoelastic behavior of DGEBA-MCDEA epoxy resin. Polym Bull 48:75–82
28. Terekhina S, Fouvrya S, Salviaa M, Bulanov I (2010) An indirect method based on fretting tests to characterize the elastic properties of materials: application to an epoxy resin RTM6 under variable temperature conditions. Wear 269:632–637
29. Deng S, Hou M, Ye L (2007) Temperature-dependent elastic moduli of epoxies measured by DMA and their correlations to mechanical testing data. Polym Test 26:803–813
30. Maxwell IA, Pethrick RA (1983) Dielectric studies of water in epoxy resins. J Appl Polym Sci 28(7):2363–2379
31. Mikols WJ, Seferis JC, Apicella A, Nicolais L (1982) Evaluation of structural changes in epoxy systems by moisture sorption–desorption and dynamic mechanical studies. Polym Compos 3(3):118–124
32. Ochi M, Yoshizumi M, Shimbo M (1987) Mechanical and dielectric relaxations of epoxide resins containing the spiro-ring structure. II. Effect of the introduction of methoxy branches on low-temperature relaxations of epoxide resins. J Pol Sci B Pol Phys 25(9):1817–1827
33. Tweedie CA, Constantinides G, Lehman KE, Brill DJ, Blackman GS, Van Vliet KJ (2007) Enhanced stiffness of amorphous polymer surfaces under confinement of localized contact loads. Adv Mater 19:2540–2546
34. Herbert EG, Oliver WC, Pharr GM (2008) Nanoindentation and the dynamic characterization of viscoelastic solids. J Phys D Appl Phys 41:1–9
35. Morelle X, Lani F, André S, Maxime M; Bailly C, Pardoen T (2012) The elasto-viscoplasticity and fracture behaviour of RTM6 epoxy resin. Proccedings of SAMPE Europe Student Conference, Paris, France, du 23/03/2012 au 25/03/2012)
36. Tabor D (1951) The hardness of metals. Clarendon, Oxford
37. Koch T, Seidler S (2009) Correlations between indentation hardness and yield stress in thermoplastic polymers. Strain 45(1):26–33
38. Schroeder JA, Madsen PA, Foistier RT (1987) Structure/property relationships for a series of crosslinked aromatic/aliphatic epoxy mixtures. Polymer 28:929–940
39. Odegard GM, Bandyopadhyay A (2011) Physical aging of epoxy polymers and their composites. J Polym Sci B Polym Phys 49(24):1695–1716
40. Bauwens J (1972) Relation between the compression yield stress and the mechanical loss peak of bisphenol-A-polycarbonate in the b transition range. J Mater Sci 7:577–584